Available online at www.sciencedirect.com
ScienceDirect
Journal of Power Sources 171 (2007) 617–625
JOURNAL OF POWER SOURCES
www.elsevier.com/locate/jpowsour

Experimental analysis and modeling for a circular-planar type IT-SOFC

S. Bedogni [a], S. Campanari [b,*], P. Iora [c], L. Montelatici [a], P. Silva [b]

[a] *Edison SpA, Research and Development, Foro Buonaparte 31, 20121 Milano, Italy*
[b] *Dipartimento di Energetica, Politecnico di Milano, P.za L. da Vinci 32, 20133 Milano, Italy*
[c] *Dipartimento di Ingegneria Meccanica e Industriale, Università di Brescia, Via Branze 38, 25123 Brescia, Italy*

Received 13 April 2007; received in revised form 13 June 2007; accepted 1 July 2007
Available online 17 July 2007

Abstract

This work presents an experimental analysis of circular-planar type intermediate-temperature solid oxide fuel cells, and the interpretation of the experimental results with a finite volume model. The model is developed to generate cell mass and energy balances and internal cell profiles for all the relevant thermodynamic or electrochemical variables, and includes a fluid-dynamic analysis focusing on the investigation of the cell internal flow conditions. Experiments have been carried out at the Edison laboratories, where several single cells fuelled with hydrogen were subject to polarization curve analysis and internal temperature measurements. The model is calibrated and validated over experimental voltage–current data, provides information on cell internal losses and demonstrates the capacity of predicting the single cell behavior and overall energy balances when changing significantly the cell operating conditions. The discussion also addresses the effects of diffusion losses appearing in the experiments carried out at high current output and low fuel hydrogen content.

Keywords: SOFC; IT-SOFC; Model; Experiment; Circular-planar

1. Introduction

Detailed investigation of fuel cell thermal and electrochemical behavior is recognized as a useful tool for the discussion of fuel cell-based system performances, especially when dealing with non-standard FC operating conditions (e.g. with variable inlet flow conditions, variable cell operating conditions and partial load simulations) [1–5]. Experiments allow to investigate such aspects, while computer simulation is often used to extend the possibility of analyzing and understanding the cell behavior. Among the different approaches available for a detailed fuel cell analysis, the finite volume method conjugates advantages in terms of flexibility, reasonable accuracy and (mostly with respect to computational fluid-dynamic codes or CFD simulations) short computational time [6–8].

In this work we propose a report of experimental tests, interpreted through a finite volume model, for a circular-planar type intermediate-temperature solid oxide fuel cell (IT-SOFC), based on the Hexis design [10].

Experiments have been carried out at the Edison laboratory facility of Trofarello [11], where several cells have been tested with hydrogen as fuel, developing polarization curves and measurement of cell internal temperatures under different air and fuel utilization rates.

The model calculates electrochemical and thermal balances, yielding cell internal temperature and flow composition profiles, fuel and oxidant utilization, cell power output and cell voltage or current output (depending on the calculation option). The electrochemical analysis evaluates the cell losses by mean of a total resistance term, depending on few coefficients which have been calibrated over available experimental results, while the thermal analysis is based on a separate fluid-dynamic calculation of cell internal heat transfer conditions.

The model shows the capacity of predicting the cell behavior and overall energy balances under the experimented cell operating conditions, providing a support for the interpretation of the experimental results. Although all the experiments and simulations are limited to single cells and are based on the use of hydrogen as fuel, the model includes the possibility of simulating the operation with natural gas or partially reformed

Abbreviations: PEM, polymer membrane electrolyte fuel cell; PEN, positive electrode, electrolyte and negative electrode structure; SOFC, solid oxide fuel cell.

* Corresponding author. Tel.: +39 02 2399 3862; fax: +39 02 2399 3940.
E-mail address: stefano.campanari@polimi.it (S. Campanari).

0378-7753/$ – see front matter © 2007 Elsevier B.V. All rights reserved.
doi:10.1016/j.jpowsour.2007.07.014

Nomenclature

A	area (m^2)
F	Faraday's constant: 96,487 C mol^{-1}
h	specific enthalpy (J mol^{-1})
i	cell current (A)
n_i	molar flow of specie i (mol s^{-1})
P	pressure (Pa)
r	cell radial coordinate (m)
R	overall cell resistance (Ω)
R_g	universal gas constant: 8.314 J mol^{-1} K^{-1}
T	temperature (K)
U_a	oxidizer utilization
U_f	fuel utilization
V	cell voltage (V)
V_{Nersnt}	Nernst cell potential (V)
X_i	molar fraction of specie i
σ	standard deviation (mV)

Subscripts

amb	ambient
c	cathodic air
cat	cathode
ext	external
f	fuel
int	internal
loc	local
r	cell radial coordinate (m)
s	solid structure (anode, cathode, electrolyte)

Superscripts

re	reacted
pr	produced

syngas, which will be investigated in future works together with an analysis of the cell performance when assembled into a stack.

2. Cell description and model assumptions

The model has been developed to simulate a circular-planar type IT-SOFC (Fig. 1) by a finite-volume approach [5,7]. The experimented cells are manufactured by H.C.Stark-InDEC B.V., and are made of an annulus shaped membrane (composed by the electrolyte and electrodes layers, often referred to as PEN structure), over which, on both sides, an array of parallelepiped type separators with edge of 1.5 mm and height of 0.8 mm is placed (Fig. 1). Internal and external diameters are 10 and 78 mm, respectively. Shape and position are consequences of structural and manufacturing needs. Separators are required in order to keep the PEN solid structure detached from the interconnects, identifying two distinct zones where air and fuel flow. In the cell stack configuration air is fed externally and is first preheated within the preheating channel (Fig. 2a). Fuel enters from the center of the annulus, then flows radially to the external side of the fuel cell with a co-flow arrangement with respect to the preheated air.

From the point of view of the calculation grid, the fuel cell is divided radially in a user-defined number of sections as shown in Fig. 2a and b. For each section the electrochemical and thermal equations discussed in the following paragraphs are progressively solved with an iterative approach.

Simulation is performed with the following assumptions:

- Stationary conditions.
- Uniform cell voltage (isopotential electrode surfaces).
- Assigned temperature profile of the PEN structure.

The last assumptions reflect the necessity to simulate single-cell performances, where the fuel cells are tested within a temperature-controlled environment discussed in the following sections.

Input data for the simulation are:

- Number of cell radial sections.
- Cell geometry (internal and external diameter, channels height and PEN structure thickness).
- Inlet fuel and air flow thermodynamic properties (T, P) and chemical compositions.

The model generates chemical concentration profiles and yields reactant utilization and cell power output. Two calculation options are allowed: the first, given the cell voltage, where the calculation is performed directly (or explicitly), as discussed in the following; the second, given the cell current (or current density given the cell active area), where the calculation follows an iterative procedure based on a first trial voltage value.

2.1. Electrochemical model

Usual finite volume modeling requires the integration of an electrochemical model with a thermal model [5–8], where the electrochemical model is first solved with a tentative temperature profile, yielding values of chemical species fluxes, cell current and electric power output. Results are then passed to the thermal model, repeating the process until convergence is reached according to a user-defined residual error. The work presented here focuses on the simulation of single cells, where the temperature profile is assigned, thus allowing a direct calculation of the electrochemical model.[1]

The electrochemical model calculates for each cell section (Fig. 3) the current power output and the molar compositions of cathode and anode flows. Thanks to the cylindrical symmetry of the cell configurations, each section is made of three sub-elements or finite volumes:

- Fuel (Fig. 3 shows only H_2 for clarity), on the anode side.
- Solid, made by the anode–electrolyte–cathode structure.
- Oxidizer (air), modeled as an O_2/N_2 mixture.

[1] In a future work, specifically dealing with the simulation of IT-SOFC stacks, the thermal model will be addressed in detail.

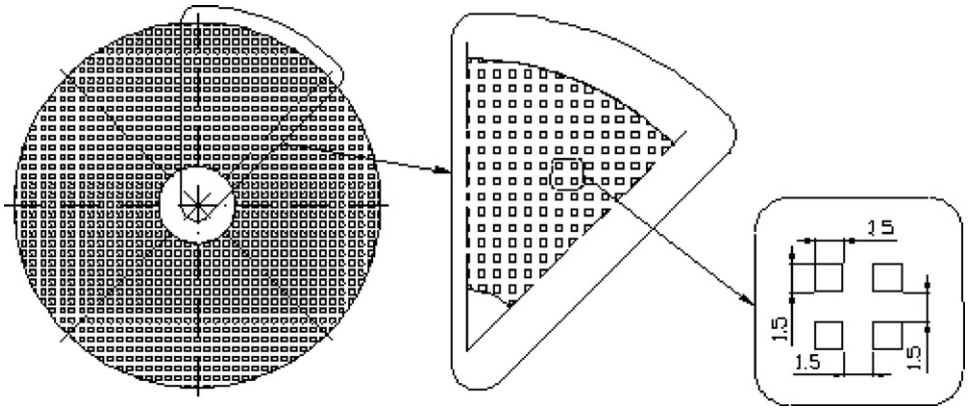

Fig. 1. Fuel cell geometry (view from the top; lengths in mm).

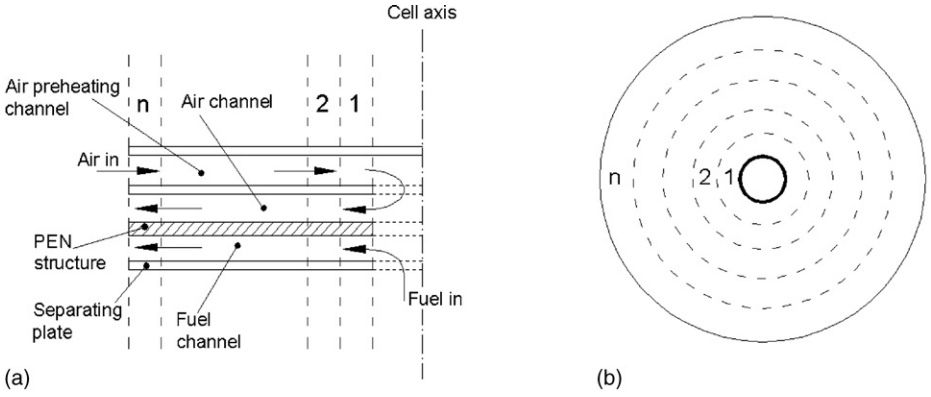

Fig. 2. (a) Fuel cell cross-section. (b) Fuel cell radial grid subdivision.

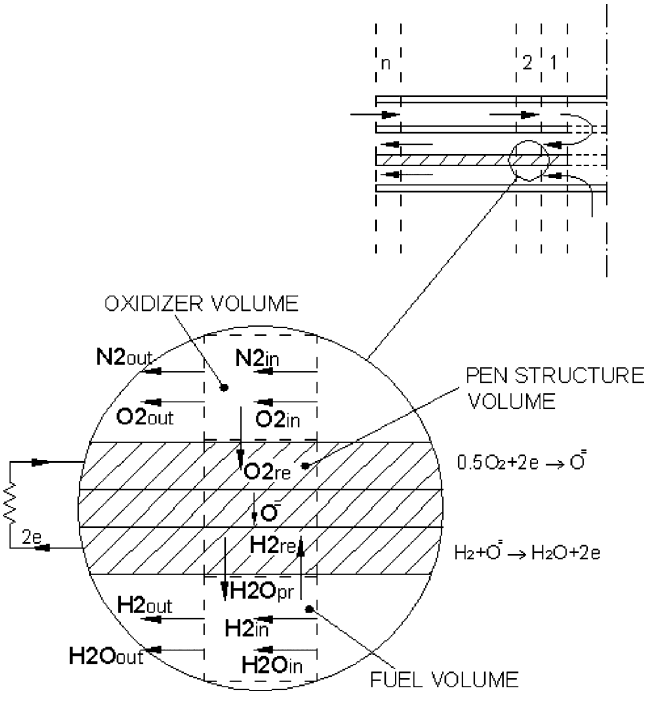

Fig. 3. Principles of the electrochemical model.

In each section, calculation is based on inlet flow compositions known by the previous section, with the exception of the first one that uses the assigned input conditions. Once the reactant compositions are known, cell local current is calculated by:

$$i_{\mathrm{loc}}\,(\mathrm{A}) = \frac{V_{\mathrm{Nernst}} - V_{\mathrm{loc}}}{R_{\mathrm{loc}}} \tag{1}$$

as a function of the following local variables: V_{Nernst} or ideal potential, V_{loc} or actual potential and R_{loc} the overall cell resistance, accounting for cell internal losses.

The Nernst potential V_{Nernst} is calculated by:

$$V_{\mathrm{Nernst}}\,(\mathrm{V}) = E^0 + \frac{R_{\mathrm{g}} T_{\mathrm{s}}}{2F} \times \left[\ln\left(\frac{X_{\mathrm{H_2}} X_{\mathrm{O_2}}^{0.5}}{X_{\mathrm{H_2O}}} \right) + \ln\left(\frac{P_{\mathrm{cat}}}{P_{\mathrm{amb}}} \right)^{0.5} \right] \tag{2}$$

with X_i the molar fractions inside each finite volume (inlet conditions) and $E^0 = 1.2723 - 2.7645 \times 10^{-4}$, T_s the ideal voltage for hydrogen oxidization at ambient pressure, expressed as a function of temperature at cell reaction sites [9,20].

Following a simplified approach already used by other authors [12,13], cell resistance R_{loc} is assumed to have the following temperature dependence:

$$R_{\mathrm{loc}}\,(\Omega) = \frac{Z \exp\left(\Delta E / B T_{\mathrm{s}}\right)}{A_{\mathrm{loc}}} \tag{3}$$

where T is the local PEN temperature, B the Boltzmann constant, $\Delta E = 0.63$ eV the activation potential assumed according to Refs. [12,14,19] and A_{loc} is the local area of the considered cell section.

The choice of lumping together the polarization effects in one equivalent resistance allows to perform an effective model calibration without the necessity of knowing detailed cell material information (e.g. electrochemical and gas diffusion properties, micro-scale properties). Such information are not available in the open literature for this kind of FC; indeed they would be necessary to correctly individuate the single polarization contributions in terms of activation, ohmic and diffusion losses, as performed in previous works for other SOFC geometries [5].

Some counterparts of this simplified approach, in terms of model accuracy and calibration issues, are addressed in the following sections, where it is discussed to extend Eq. (3) by considering an additional loss term specifically related to diffusion losses, which have demonstrated their importance in the experiments featuring high currents and/or low hydrogen fuel content.

Once the current i is calculated from Eq. (1), the number of moles of hydrogen and oxygen consumed in each section, as well as the generated water can be determined as follows:

$$n^{re}_{H_2} = \frac{i}{2F}; \quad n^{re}_{O_2} = \frac{i}{4F}; \quad n^{pr}_{H_2O} = \frac{i}{2F} \tag{4}$$

It is finally possible to find the composition of the flows given to the next cell section as

$$n^{i+1}_{H_2} = n^{i}_{H_2} - n^{re}_{H_2}; \qquad n^{i+1}_{O_2} = n^{i}_{O_2} - n^{re}_{O_2};$$
$$n^{i+1}_{H_2O} = n^{i}_{H_2O} + n^{pr}_{H_2O} \tag{5}$$

The model is developed in Fortran code [16]. In principle, the model has been developed to consider different possible fuels, including hydrogen as well as natural gas or partially reformed syngas. For the latter cases, reforming and water gas shift reactions generate H_2 and CO from the hydrocarbons and steam contained in the fuel flow, with a mechanism modeled as discussed in previous works [5,7]. However, cell experimental testing and model validation performed in this work have been developed using pure hydrogen as fuel.

From the point of view of boundary conditions, we consider here to simulate isolated cells, inserted in a test bench, where a user-defined temperature profile can be assigned to the cell PEN structure along the radial direction. The temperature profile depends on the oven heating capabilities and on the cell thermal balances, and in the experiments carried out here has demonstrated to be rather smooth, i.e. the PEN is kept at an approximately constant temperature of 800 °C by the combined effect of the oven heating and by the thermal inertia of the air mass flow rate employed in the experiments. As already mentioned, the PEN temperature is directly assigned to the electrochemical model.

2.2. Gas flow fluid-dynamic conditions

A separate detailed investigation of the gas flow conditions inside and outside the fuel cell (air and fuel flows) has been carried out with a finite volume analysis based on computational fluid dynamics (CFD) software (Fluent®) [22].

The analysis was originally carried out to investigate the heat transfer conditions inside the fuel cell [23], and some results regarding the gas flow arrangement are reported here because of their relevance with respect to the interpretation of the cell experimental behavior. Gas flow shows interesting peculiarities due to the presence of the array of parallelepiped type separators shown in Fig. 1, leading to the formation of preferential flow paths and stagnation areas, which can be seen in Fig. 4.

The presence of stagnation areas, where it occurs a low reactant circulation, and preferential gas paths, causes a non-uniform distribution in the reactant utilization and in the current density, negatively influencing the cell performances. Moreover, the gas

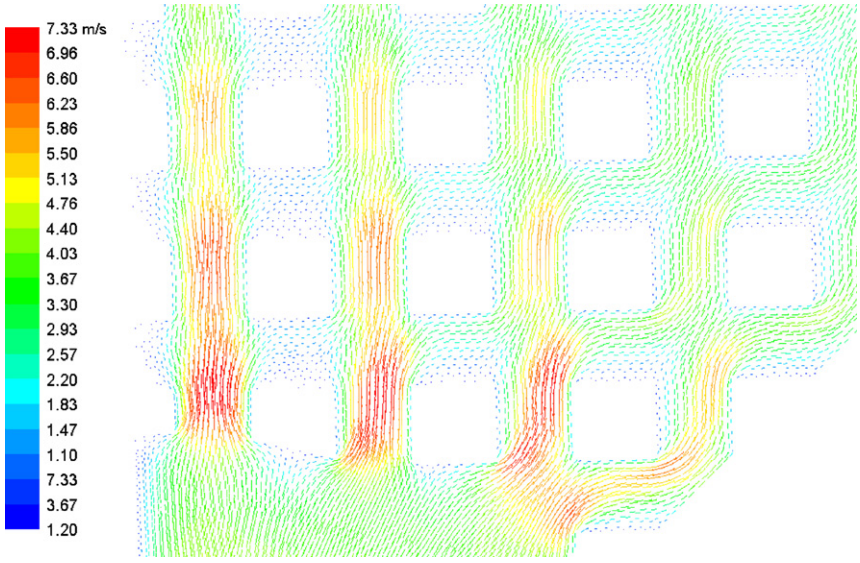

Fig. 4. Velocity vectors, in a mean horizontal section of the channel, at the cell inlet, under typical operating conditions [23].

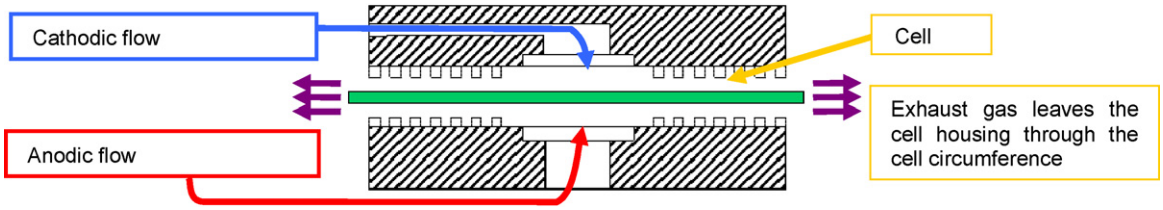

Fig. 5. Gas distribution on the electrode surfaces in the single cell test bench.

flow condition shown in Fig. 4 considerably changes with the reactant mass flow rate (as a general rule, increasing the mass flow rate yields an extension of stagnation areas and concentrates the flow over the preferential paths), variably affecting the cell performance. A detailed analysis of this issue can be found in Ref. [23].

3. Experimental analysis

Several experimental tests have been conducted on circular-planar IT-SOFC single cells. A preliminary set of tests yields a thermal characterization of the cell inner channels and PEN solid layer, showing the validity of axial symmetry assumption for the simulation model. A second experimental campaign has been carried out in order to obtain a complete characterization of the cell electrical behavior through voltage–current measures. This phase allowed to perform a calibration of the model over experimental data, as explained in the following paragraphs.

3.1. The test facility

The fuel cell facility is located at the Edison R&D Center, Trofarello (TO). The lab features five independent test benches, allowing single cell and small stacks test activities, both on SOFC (tubular and planar design) and PEM technologies [11,24].

The lab activities mainly consist of tests for the cell characterization under different operating conditions (temperature, gas flows and load) and long-term tests aimed at assessing the cell durability.

3.1.1. Test stand description

The planar SOFC test stand consists of an oven hosting the cell housing, an electronic load, a gas flow regulation system and a software application, which controls the above-mentioned sub-units and performs the test data acquisition.

The integration of the stand sub-units was designed and realized by the Edison R&D staff, based on the experience gained through the realization and tuning of other test benches previously developed at the fuel cells laboratory.

The oven, hosting the cell housing, is the core element of the stand.

The cell housing has no seals to separate the anode and cathode compartments; for the purpose of testing single cells, the two reactants are ducted to the center of the electrode surfaces through the supporting ceramic disks, then spread radially along the whole active area by means of channels dug on the same disks (Fig. 5). The test configuration for a single cell is then coherent with the fuel cell model discussed above (Figs. 2 and 3), with the simplification derived from the absence of the air-preheating channel.

After exiting the fuel cell, unused hydrogen from the anode exhaust burns with the ambient air; this oxidation occurs right outside the cell periphery.

Each current collector is composed of two thin metallic gauzes placed one upon the other between the cell and the corresponding ceramic disk. The gauze material is nickel at the anode, and platinum at the cathode.

Current is collected through several platinum wires placed in the ceramic channel and welded to the gauzes; the wires are then twisted together to connect to the power leads of the electronic load, which are also made in platinum.

After placing the cell on the anodic support, the cathodic disk is placed on top of the cell (Fig. 6); the oven is then completely closed.

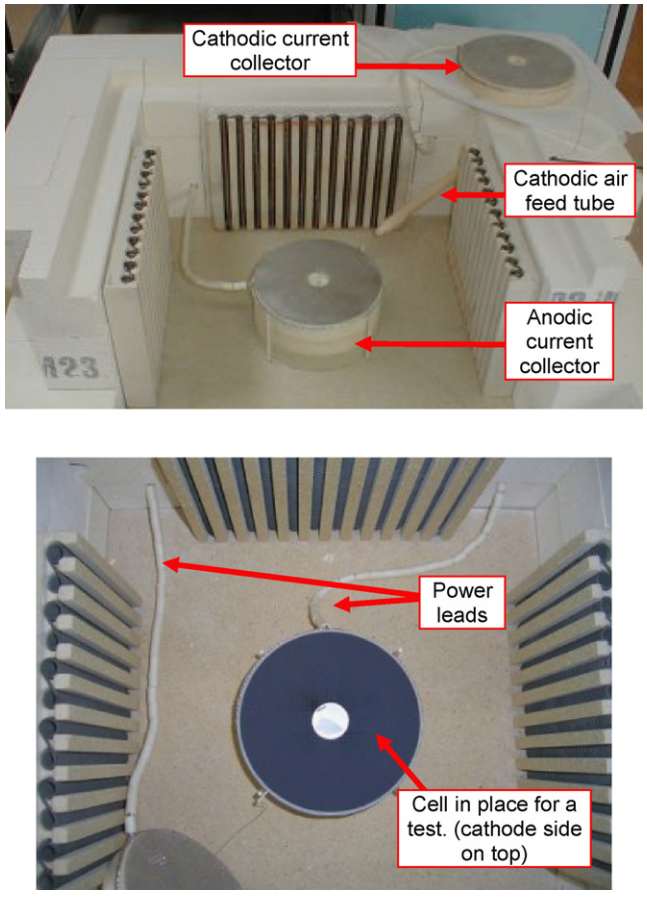

Fig. 6. Oven and cell housing.

The cell is loaded with weights by means of a ceramic tube laying on the cell housing and extended across the oven cover wall, up to the external side; by this way the cell housing is compressed in order to get a good electric contact and sufficient gas-tightness.

The oven, built with refractory bricks, is heated by means of electric resistances; several thermocouples are used to monitor the oven temperature distribution, especially around the cell housing. The "hot module" consisting of the oven and the cell housing has been provided by the Energy Research Centre of the Netherlands (ECN).

The power generated by the cell is fed to the power circuit made by the series of the electronic load and an auxiliary voltage supplier; the latter is needed to increase the overall circuit voltage and to allow the load to work properly, due to the low voltage/current ratio provided by a single cell.

The gas flow is controlled by four thermal mass flow regulators: two are dedicated to an accurate tuning of the hydrogen flow in the range of interest for the tests, while the other two are respectively used to control the nitrogen flow, used in the anodic flow to allow variations in the hydrogen concentration, and air, which is the cathodic gas.

A further gas line is dedicated to a nitrogen–hydrogen mixture (3% hydrogen, balance nitrogen) which is used in any emergency situation to maintain a reducing environment on the anode side of the cell while the oven cools down, preventing the risk of nickel oxidation.

The control and data acquisition software allows to set all the parameters required by the test (i.e. gas flows, temperatures and current), with the possibility of designing long term automatic tests to follow specific profiles (polarizations, temperature ramps and galvanostatic steps).

3.2. Test procedures

The test period lasts a minimum of one week, as the cell needs to be heated up and cooled down with low temperature gradients (<30 °C h^{-1}).

Moreover, a preliminary activation procedure is carried out once for each new cell, lasting about two days and consisting of two stages:

- anode reduction: after preheating at 750–800 °C, an increasing hydrogen flow is fed to the anode, aiming to reduce the nickel oxide.
- a 48 h galvanostatic step, after which the cell is ready to undergo the planned tests.

In some cases, tests have been carried out for long periods (e.g. 1000 h), in order to investigate the cell durability and performance decay issues (Fig. 7).

The majority of the other tests have been developed aiming to describe the electrical performances of the cell through voltage–current polarization curves, obtained with different fuel compositions and mass flow rates.

Tests are performed with imposed current and measured cell voltage, for different fuel compositions and mass flows feeding the cell anode. Different fuel compositions are obtained mixing together pure hydrogen and nitrogen gas currents with variable proportions before entering the cell. The experimental apparatus also includes a saturator device for humidification of the fuel gas: the gas mixture is injected in a water vessel kept at a constant temperature of 29 °C. The molar fraction of water in the fuel gas after saturation depends on water temperature and in all cases is close to 4% [21]. The internal temperature of the cell is measured through two thermocouples inserted in the anode and cathode channels at 2/3 of the cell radius. As already mentioned, the temperature profile on the PEN structure is kept almost uniform at 800 °C thanks to the action of the oven heat supply and the thermal inertia of the air mass flow rate employed in the experiments.

3.3. Test results

Table 1 reports the experimental characteristic curves obtained with different fuel gases: the corresponding

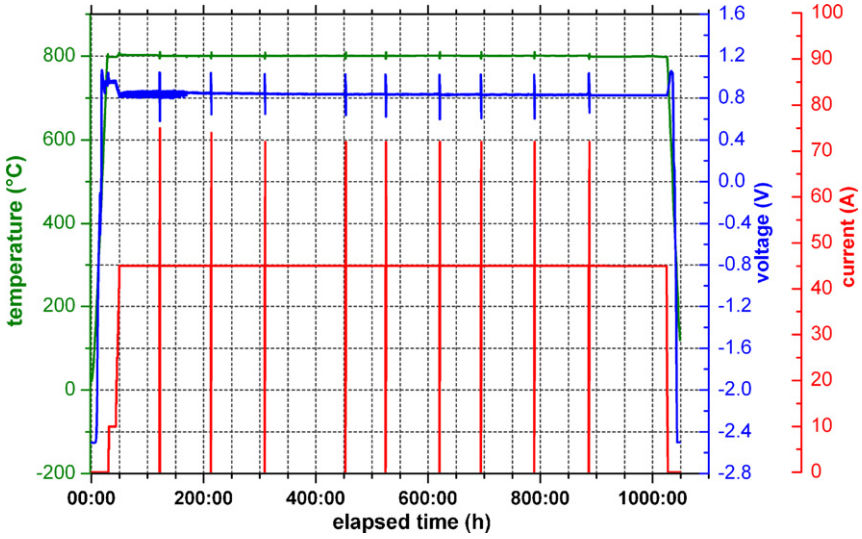

Fig. 7. Example of complete report of a planar SOFC test. The vertical lines are periodical polarization tests.

Table 1
Experimental values of cell voltage as a function of imposed current for different fuel compositions and mass flow rates (see Table 2)

Current (A)	V_{ref} (V)										
	1[a]	2[a]	3[a]	4[a]	5[a]	6[a]	7[a]	8[a]	9[a]	10[a]	11[a]
0	1.007	1.001	0.997	0.993	0.983	0.981	1.002	1.015	0.997	1.001	1.008
1	0.993	0.986	0.981	0.975	0.963	0.960	0.985	1.002	0.980	0.986	0.992
2	0.981	0.972	0.966	0.959	0.946	0.942	0.971	0.991	0.964	0.972	0.978
3	0.969	0.960	0.953	0.944	0.929	0.925	0.957	0.980	0.950	0.960	0.964
4	0.958	0.948	0.940	0.931	0.914	0.910	0.945	0.970	0.937	0.948	0.953
5	0.948	0.937	0.928	0.917	0.900	0.894	0.933	0.960	0.924	0.937	0.941
6	0.937	0.926	0.917	0.905	0.885	0.880	0.922	0.951	0.912	0.926	0.931
7	0.928	0.916	0.906	0.893	0.871	0.865	0.912	0.942	0.901	0.916	0.920
8	0.919	0.906	0.895	0.881	0.858	0.850	0.901	0.934	0.889	0.906	0.910
9	0.910	0.896	0.885	0.869	0.845	0.835	0.891	0.925	0.878	0.896	0.901
10	0.901	0.887	0.874	0.858	0.831	0.820	0.882	0.918	0.867	0.887	0.891
15	0.859	0.841	0.825	0.800	0.745	0.712	0.834	0.880	0.814	0.841	0.848
20	0.820	0.798	0.775	0.730	0.416		0.789	0.847	0.756	0.798	0.807
25	0.783	0.753	0.717	0.547			0.742	0.816	0.668	0.753	0.768
30	0.745	0.701	0.608				0.683	0.786		0.701	0.728
35	0.704	0.619					0.572	0.757		0.619	0.683
40	0.653										0.620

[a] Curve number.

Table 2
Fuel mass flow rate and fuel composition (the water content is complementary to 100%) used for experimental characterization of the cell

Curve number	Fuel mass flow rate ($g\,s^{-1}$)	H_2 (vol. %)	N_2 (vol. %)
1	0.00342	76	20
2	0.00514	60	36
3	0.00626	50	46
4	0.00737	40	56
5	0.00850	30	66
6	0.00757	31	65
7	0.00755	51	45
8	0.00748	74	22
9	0.00589	48	48
10	0.00783	48	48
11	0.01170	48	48

Airflow rate is always set to 0.0324 $g\,s^{-1}$.

fuel gas composition and mass flow rates are given in Table 2.

As it can be observed in Table 1, voltage at open circuit (VOC) and maximum cell current can be in some way related to hydrogen concentration at the anode.

More specifically, the fuel mass flow seems to have a small but significant influence on the VOC, also when the fuel composition is constant (see for instance cases 9–11). Such variation suggests that the VOC is somehow influenced by the flow field in the anodic channels, probably due to the local flow non-uniformity evidenced in the fluid-dynamic analysis discussed in Ref. [23] and partially reported at Section 2.2 above.

4. Model calibration

A model calibration has been performed utilizing data from the experiments of Table 1.

Calibration allowed to find a set of parameters that minimizes the difference between calculated and experimental data. Parameter Z in Eq. (3) of cell resistance adopted in the calculation model is $3.4 \times 10^{-8}\,\Omega\,m^2$.

The comparison of experimental VOC tension and Nernst ideal potential, calculated by Eq. (2), shows a constant gap of about 58 mV, which was not expected by theory.

The difference can be probably explained by the existence of parasitic currents between electrodes, depending on specific cell manufacturing features, which are rather difficult to be evaluated. However, the difference is almost constant in all cases, so that the calculated voltage in the program could be corrected with a simple offset parameter of 58 mV.

Following this additional assumption, the first calibration yields an average absolute difference between model prediction and experimental results (average over the 11 calibration curves) limited to 1% for currents up to 10 A, 2% up to 20 A and increasing up to 5–6% at 30–40 A.

Despite the good general accordance between model and experimental data, this first calibration showed some difficulties in the high current regions of some polarization curves, limited to the cases where the hydrogen content of the fuel mixture is low.

To better focus this aspect, Figs. 8–10 represent examples of comparison between experimental and calculated values (continuous curves, label "Calculated 1"), respectively for the cases 1, 3 and 5 of Table 2.

The accordance between the model and the experiments is always good in the first figure (referred to case 1 in Table 2, but substantially representative also of cases 2,8,10 and 11, not shown here for brevity), while some discordance at high current begins to appear in Fig. 9 (referred to case 3; the same would happen with the results of cases 6,7 and 9 of Table 2) and becomes rather large in Fig. 10 (referred to case 5, which is the worst

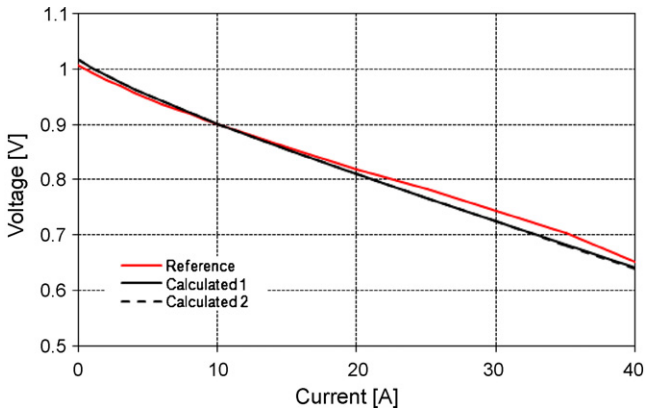

Fig. 8. Experimental and calculated values for case 1.

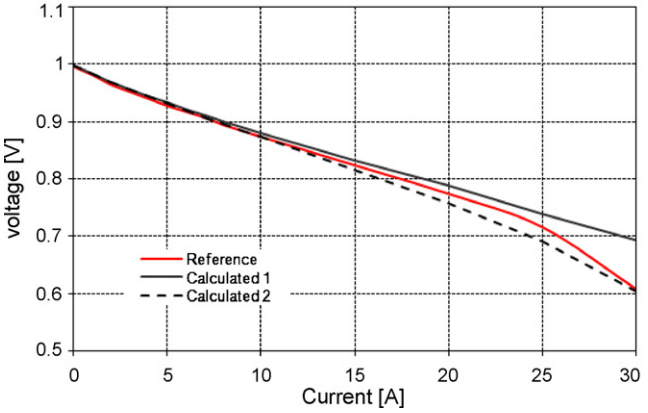

Fig. 9. Experimental and calculated values for case 3.

condition; a similar but less critical situation would appear with the results of cases 4 and 6).

The main difference among these cases is that going from Figs. 8 to 10, the fuel mass flow increases and the hydrogen content becomes lower; it is possible to conclude that the model shows good accuracy in predicting the experimental curves in all cases with higher hydrogen concentration, while it yields some difficulties at high current/low hydrogen content.

The phenomenon can be explained considering diffusion losses, whose effect becomes important when hydrogen concentration at the anode is rather low and the fuel utilization factor (proportional to the current output) is high. As mentioned in paragraph 1.1, the algorithm adopted in the program does not include a mathematical model for a separated description of diffusion losses, but all the polarization losses are lumped in an equivalent resistance term, so that the diffusion loss effect cannot be captured by the simulation.

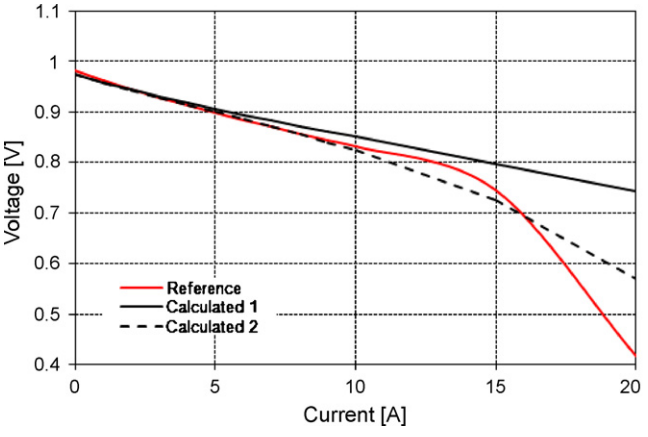

Fig. 10. Experimental and calculated values for case 5.

Aiming to partially overcome this issue, we have considered to add a second resistance term to Eq. (3), accounting for diffusion effects with an approach based on the introduction of a limiting fuel utilization, which turns into a limitation in the hydrogen consumption. The new expression of the cell overall resistance is then:

$$R_{\mathrm{loc}}\,(\Omega) = \frac{Z\,\exp\left(\Delta E/BT_s\right)}{A_{\mathrm{loc}}} + k\,\log\left(1 - \frac{(m_{\mathrm{H_2,in}} - m_{\mathrm{H_2,loc}})/m_{\mathrm{H_2,in}}}{Uf_{\mathrm{lim}}}\right) \quad (6)$$

where the terms Z and B, remain the same discussed at Section 2.1, T_s is the local PEN temperature, K is an external parameter and Uf_{lim} is the limiting fuel utilization. At the numerator of the new term, $m_{H_2,in}$ is the mass flow of hydrogen entering the fuel cell, while $m_{H_2,loc}$ is the local mass flow along the cell radius.

A further calibration has been carried out, yielding the results shown with the dotted lines in Figs. 8–10 (label "Calculated 2"), where Uf_{lim} is always set to 80% and best fitting results are obtained when K is calculated following the empirical expression:

$$K\,(\Omega) = 0.688\,\log(X_{\mathrm{H_2,in}}) + 0.187 \quad (7)$$

where $X_{H_2,in}$ is the molar fraction of hydrogen entering the fuel cell.

The additional term of Eq. (6) becomes progressively relevant when the fuel utilization approaches 80%, which has been set as a limit value, never reached in the experiments.

The new equation yields good results in the case of Fig. 9, where the standard deviation between experimental and calculated polarization curves (calculated over the entire diagram) remains below 40 mV versus 92 mV of the first calculation. As it could be expected, thanks to the logarithmic form of the term added in Eq. (6), the situation remains also good in Fig. 8 where the two equations yield similar results and the standard deviation σ is about 40 mV in both cases.

The use of Eq. (6) allows also a significant reduction of the standard deviation for case 5 in Fig. 10, which represents the worst condition, now reaching $\sigma \cong 150$ mV versus about 330 mV for the same case calculated in the first manner. Trying to further reduce the error for case 5 considerably worsen the good results obtained in Figs. 8 and 9, so that this final condition can be considered a reasonable calibration compromise among the different cases.

Finally, in all experiments it can be noted that there is no evidence of a convex behavior of the curves in the vicinity of the VOC tension, as can be expected for an intermediate or high-temperature fuel cell, where activation losses are typically low.

The result is captured in all the simulations, independently of the use of Eq. (3) or Eq. (6) for the cell resistance loss.

5. Conclusions

In this work we have presented experimental results of testing over circular-planar type intermediate-temperature solid oxide fuel cells, based on the Hexis design [10], interpreted through a finite volume model.

The model has been calibrated over the results of experiments carried out at the Edison laboratory facilities, where several cells have been tested with hydrogen as fuel, developing polarization curves and measurement of cell internal temperatures under different air and fuel utilization rates. The work reports the test modalities and the results of the experiments, discusses the comparison between the model simulations and the experimental results, and evidences the dependence of the cell performances on the operating conditions. The comparison demonstrates the capacity of the model to predict the cell behavior and overall energy balances when changing significantly the cell operating conditions, and discusses the effects of diffusion losses appearing in the experiments carried out at high current output and low fuel hydrogen content.

References

[1] D. Stephenson, I. Ritchey, ASME paper 97-GT-340, June 1997.
[2] S. Campanari, ASME J. Eng. Gas Turb. Power 122 (2000) 239–246.
[3] E. Riensche, et al., J. Power Sources 86 (2000) 404–410.
[4] L. Magistri, R. Bozzo, P. Costamagna, A. Massardo, Simplified versus detailed SOFC reactor models and influence on the simulation of the design point performance of hybrid systems, in: Proceedings of the ASME Turbo Expo 2002, GT-2002-30653, Amsterdam, 2002, June.
[5] S. Campanari, P. Iora, J. Power Sources 132 (2004) 113–126.
[6] Recknagle, et al., J. Power Sources 113 (2003) 109–114.
[7] S. Campanari, P. Iora, Fuel cell–from fundamentals to systems 5 (1) (2005) 34–51.
[8] S. Campanari, P. Iora, ASME J. Fuel Cell Sci. Technol. (2007), ISSN:1550-624X, in press.
[9] Anon, Fuel Cell Handbook, 7th ed., U.S. Department of Energy (DOE), 2004.
[10] R. Diethelm, P. Hardegger, H. Raak, The Fuel Cell Home, July 2–6, Lucerne, 2001.
[11] S. Bedogni et al., Fuel Cell Sci. Technol., Torino, September 13–14, 2006.
[12] J. Palsson, A. Selimovic, P. Hendriksen, Intermediate temperature SOFC in gas turbine cycles, in: Proceedings of ASME TURBO EXPO 2001, June 4–7, New Orleans, Louisiana, USA, 2001.
[13] P. Iora, S. Campanari, Parametric analysis of a planar SOFC model with geometric optimization, in: 6th European SOFC Forum, Lucerna, 2004, July.
[14] P. Costamagna, K. Honegger, J. Eletrochem. Soc. 145 (11) (1998) 3995–4007.
[16] IMSL Math Library in “Compaq Visual Fortran”, Vol. 1, p.846, Compaq Computer Co., 2000.
[19] R.H. Perry, W. Green, Perry’s Chemical Engineer’s Handbook, 7th ed., McGraw-Hill, 1997.
[20] A. Bejan, Advanced Engineering Thermodynamics, Wiley, 1988.
[21] R.C. Reid, J.M. Prausnitz, B.E. Poling, The Properties of Gases and Liquids, 4th ed., McGraw-Hill, New York, 1987.
[22] Fluent 6.2.16 Manual, Fluent Inc., 2005.
[23] S. Campanari, P. Iora, A. Lucchini, M. Romano, Thermofluidynamic analysis of circular-planar type IT-SOFCs, in: Proceedings of the ASME Fifth International Conference on FC Science, Engineering and Technology, New York, 2007.
[24] R. Barrera, S. Bedogni et al., GEI 2005 Spoleto, 11–15 September 2005.